The Canadian Mineralogist
Vol. 47, pp. 625-634 (2009)
DOI: 10.3749/canmin.47.3.625

THE ATOMIC STRUCTURE OF $(H_3O)Fe^{3+}(SO_4)_2$ AND RHOMBOCLASE, $(H_5O_2)Fe^{3+}(SO_4)_2 \cdot 2H_2O$

RONALD C. PETERSON§

Department of Geological Sciences and Geological Engineering, Queen's University, Kingston, Ontario K7L 3N6, Canada

ELENA VALYASHKO

Department of Civil Engineering, Royal Military College, Kingston, Ontario K7K 7B4, Canada

RUIYAO WANG

Department of Chemistry, Queen's University, Kingston, Ontario K7L 3N6, Canada

ABSTRACT

The atomic structure of $(H_3O)Fe^{3+}(SO_4)_2$, an important phase in the system Fe–S–O–H, has been determined by the analysis of single-crystal X-ray-diffraction data. Within the unit cell of $(H_3O)Fe(SO_4)_2$, there are three layers consisting of $Fe(SO_4)_2$ sheets parallel to (001) composed of FeO_6 octahedra and SO_4 tetrahedra sharing corners. The structure of $(H_3O)Fe^{3+}(SO_4)_2$ is very similar to that of $(H_3O)Al(SO_4)_2$ except that it is distorted from the $R\bar{3}$ arrangement of $(H_3O)Al(SO_4)_2$ to $P\bar{1}$ symmetry. The phase $(H_3O)Fe^{3+}(SO_4)_2$ has a layer spacing of 7.90 Å, which is slightly larger than the spacing for $(H_3O)Al(SO_4)_2$ (7.75 Å). This increase is a direct result of the mean Fe^{3+}–O bond length (1.976 Å) being longer than the mean Al–O bond length (1.879 Å). The longer Fe^{3+}–O bond length also causes the array of oxygen atoms formed by the apices of the sulfate groups that bond to the hydronium groups to be farther apart. The adjustment of the hydrogen bonding to this change results in the lower symmetry. The crystal structure of rhomboclase, $(H_5O_2)Fe^{3+}(SO_4)_2 \cdot 2H_2O$, has been refined, and the hydrogen positions have been determined for the first time. The model describing the disorder of the H_5O_2 molecule is confirmed.

Keywords: iron sulfate, rhomboclase, crystal structure, hydronium, X-ray diffraction, hydrogen bonding.

SOMMAIRE

Nous avons déterminé la structure du composé $(H_3O)Fe^{3+}(SO_4)_2$, phase importante du système Fe–S–O–H, par diffraction X avec données prélevées sur monocristal. Dans la maille élémentaire de $(H_3O)Fe(SO_4)_2$, il y a trois feuillets $Fe(SO_4)_2$ parallèles à (001) composés d'octaèdres FeO_6 et de tétraèdres SO_4 à coins partagés. La structure de $(H_3O)Fe^{3+}(SO_4)_2$ ressemble étroitement à celle du composé $(H_3O)Al(SO_4)_2$ sauf que les distorsions favorisent une symétrie $P\bar{1}$ plutôt que l'agencement $R\bar{3}$ de la phase $(H_3O)Al(SO_4)_2$. Dans la phase $(H_3O)Fe^{3+}(SO_4)_2$, les couches ont une séparation de 7.90 Å, légèrement supérieure à la séparation analogue du $(H_3O)Al(SO_4)_2$ (7.75 Å). Cette augmentation découle directement de la longueur moyenne de la liaison Fe^{3+}–O (1.976 Å), supérieure à la liaison moyenne Al–O (1.879 Å). La longueur de la liaison Fe^{3+}–O cause aussi une plus grande distance entre les atomes d'oxygène qui représentent les sommets des groupes sulfate, et qui forment une liaison avec les groupes hydronium. L'ajustement du réseau de liaisons hydrogène qui en résulte est la cause de la symétrie plus faible. Nous avons affiné la structure cristalline de la rhomboclase, $(H_5O_2)Fe^{3+}(SO_4)_2 \cdot 2H_2O$, et nous établissons la position des atomes d'hydrogène pour la première fois. Nous confirmons le modèle déjà proposé décrivant le désordre dans la molécule H_5O_2.

(Traduit par la Rédaction)

Mots-clés: sulfate de fer, rhomboclase, structure cristalline, hydronium, X-ray diffraction, hydrogen bonding.

§ *E-mail address*: peterson@geol.queensu.ca

Introduction

Compounds with the formulae $(H_5O_2)M^{3+}(SO_4)_2 \bullet 2H_2O$ and $(H_3O)M^{3+}(SO_4)_2$ with M^{3+} = Ti, Fe, In and Al have been investigated as possible protonic conductors for use as solid electrolytes in fuel cells and other devices (Chang *et al*. 1983, Brach *et al*. 1989, Hashmi *et al*. 1992, Trojanov *et al*. 1996, Ponomareva *et al*. 2002). These materials derive their high electrical conductivity through proton translocation (Glasser 1977). Rhomboclase, $(H_5O_2)Fe^{3+}(SO_4)_2 \bullet 2H_2O$, is found in mine waste associated with szomolnokite, melanterite and copiapite (Palache *et al*. 1951). Rhomboclase has been suggested as a possible sulfate on the surface of Mars (Morris *et al*. 2005), as it precipitates from very acidic fluids, and such solutions may have existed on the Martian surface in the past.

In our work, the goal at the outset was the synthesis and study of material with the same structural and chemical properties as the mineral lausenite $[Fe_2(SO_4)_3(H_2O)_5]$. During the course of our study, Majzlan *et al*. (2005) reported the synthesis of $Fe_2(SO_4)_3(H_2O)_5$ and solved the crystal structure using high-resolution powder-diffraction data. However, during our synthesis attempts, we obtained crystals of $(H_3O)Fe^{3+}(SO_4)_2$, a phase for which the atomic structure has not been previously described and which is relevant to the Fe–S–O–H system. Although $(H_3O)Fe^{3+}(SO_4)_2$ was grown at temperatures greater than those found in most mine-waste environments, we describe its structure because it adds to our understanding of iron sulfates, and it is closely related to rhomboclase. High-temperature hydrous sulfate phases of this sort have been described from fumaroles and mine-fire situations in the past (Lausen 1928).

The crystal structure of rhomboclase has been refined in order to study the H_5O_2 molecule and compare it with the H_3O molecule observed in $(H_3O)Fe^{3+}(SO_4)_2$. The crystal structure of rhomboclase has been studied previously by Mereiter (1974), who determined the positions of the oxygen atoms of the interlayer H_5O_2 molecules. Majzlan *et al*. (2006) measured thermodynamic properties of rhomboclase and refined the positions of the non-hydrogen atoms by Rietveld refinement of X-ray powder-diffraction data.

Synthesis

In a careful and systematic study of the system Fe_2O_3–SO_3–H_2O, Posnjak & Merwin (1922) synthesized twelve different ferric sulfate phases from sulfuric acid, water and commercially available reagents with chemical formulae of $2Fe_2O_3 \bullet 5SO_3 \bullet 17H_2O$ and $3Fe_2O_3 \bullet 4SO_3 \bullet 9H_2O$. The convention of Posnjak & Merwin (1922), where the compositions of the phases are listed in terms of the molar amounts of Fe_2O_3, SO_3 and H_2O, is used in the present study. This is done to allow the plotting of neutral molar components. All phases contain sulfate, not sulfite. The experiments of Posnjak & Merwin (1922) were conducted in sealed Jena tubes placed in a resistance furnace within a steel vessel for up to several weeks, depending on the temperature. Figure 1 shows a modified phase-diagram determined by Posnjak & Merwin (1922) relevant to the present work. The synthesis of $(H_3O)Fe(SO_4)_2$ that is the subject of this study was performed in two steps. First, synthetic ferricopiapite was precipitated by mixing a saturated solution of a commercial ferric sulfate (reagent grade, 99.99%) and acetone in a proportion of 1:10 following the method of Margulis *et al*. (1973). The resulting solid was then mixed with either 14.5 or 15.4 M H_2SO_4 and placed in a Teflon-lined steel vessel (Parr bomb) of 25 mL capacity. In each case, 0.75 g of ferricopiapite and 2 mL of H_2SO_4 were used to prepare the starting mixture. Runs were placed in an oven at 140°C for 40 days. The bomb was cooled by placing it in 20°C water for 10 minutes at the end of the experiments. The resulting solid appeared as a white-yellow mass with two distinct types of crystals. One type of crystal exhibits a six-sided tabular morphology dominated by a parallelohedron modified by an apparent rhombohedron and is the subject of this study (Fig. 2). A second type of crystal was also observed that exhibits an acicular habit. Both types of crystals were separated from the solution and studied by X-ray diffraction using a 114.7 mm Gandolfi camera using Fe-filtered Co$K\alpha$ radiation. The acicular crystals were tentatively identified as $Fe_2(SO_4)_3 \bullet 6H_2O$ on the basis of optical properties [$2V$ = 79.1(2)° measured by spindle-stage methods; compare $2V$ = 80° calculated from the data of Posnjak & Merwin 1922] and stability conditions described by Posnjak & Merwin (1922). The crystals are optically twinned with the twin plane parallel to their elongation. The positions of the X-ray-diffraction peaks do not match those of the material described as lausenite by Srebrodolskiy (1974), but they closely match the powder-diffraction pattern of $Fe_2(SO_4)_3 \bullet 5H_2O$ measured by Majzlan *et al*. (2005) with the exception of two unexplained peaks at 9.45 and 8.39 Å (Table 1). These unaccounted peaks are difficult to explain as an impurity because the diffraction experiment used individual crystals attached to a fiber for the Gandolfi exposure. These additional peaks cannot be indexed using the unit cell given by Majzlan *et al*. (2005). There was not enough material to conduct a TGA analysis; the fine-scale twinning and the small size of the crystals precluded single-crystal X-ray-diffraction analysis. Further work is required to resolve these ambiguities.

The $(H_3O)Fe(SO_4)_2$ crystals exhibit a platy morphology. The X-ray-diffraction pattern closely matches the pattern for $(H_3O)Al(SO_4)_2$ (Fischer *et al*. 1996). Material with the composition $(H_3O)Fe(SO_4)_2$ was not observed by Posnjak & Merwin (1922) at 140°C on the basis of a chemical analysis of the run products. However, they did observe material with this composition at 110°C, which is the next lower

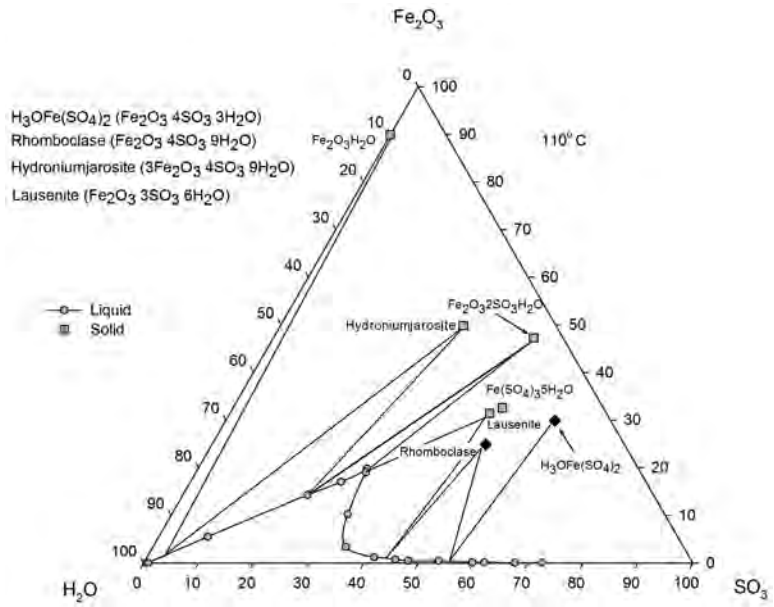

FIG. 1. The phase diagram for the system Fe_2O_3 – SO_3 – H_2O at 110°C as determined by Posnjak & Merwin (1922). The location of $(H_3O)Fe(SO_4)_2$ and rhomboclase are indicated by filled diamonds. Fluids in equilibrium with solids are indicated by circles connected by tie-lines. Lausenite, $Fe_2(SO_4)_3$•$5H_2O$, and $Fe_2(SO_4)_3$•$6H_2O$ are both plotted. Majzlan *et al*. (2005) described the atomic structure of $Fe_2(SO_4)_3$•$5H_2O$.

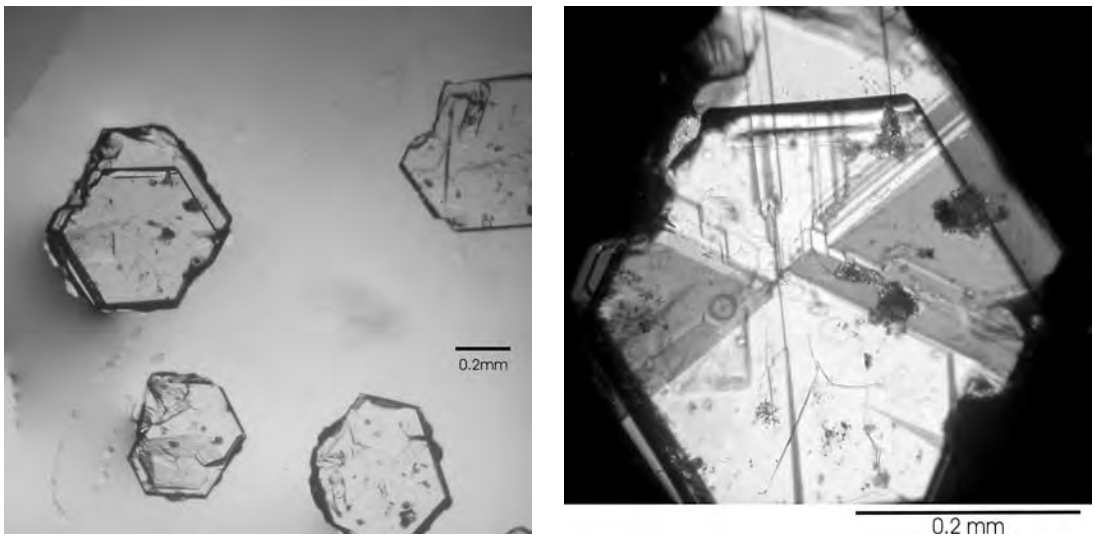

FIG. 2. a) Plane-light image of the pseudorhombohedral platy crystals of $(H_3O)Fe(SO_4)_2$. b) Cross- polarized-light image of a crystal showing twin domains of triclinic $(H_3O)Fe(SO_4)_2$.

temperature that was studied. Posnjak & Merwin (1922) described this material as very fine needles with parallel extinction, which is not consistent with flattened pseudorhombohedral morphology of the material synthesized in this study.

Determination of the Structure $(H_3O)Fe^{3+}(SO_4)_2$

A fragment of a hexagonal platy crystal that appeared not to be twinned when examined by optical microscopy was selected for study by X-ray diffraction. The colorless crystal was sealed in a mineral-oil-filled capillary. Data collection was performed on a Bruker SMART CCD 1000 X-ray diffractometer with graphite-monochromated Mo$K\alpha$ radiation ($\lambda = 0.71073$ Å), over a θ range of 5.20 to 50.00° at 25°C. No significant decay of standard diffraction-intensities was observed during the data collection.

TABLE 1. COMPARISON OF X-RAY POWDER-DIFFRACTION DATA FOR $Fe(SO_4)_3{\cdot}5H_2O$

prismatic crystals		Majzlan *et al.* (2005)	
d (Å)	I_{rel}	*d* (Å)	I_{rel}
10.56	10	10.53	8
9.45*	10		
8.39*	10		
7.67	100	7.62	100
5.52	40	5.52	29
4.90	10	4.89	19
4.73	40	4.72	8
4.59	40	4.59	9
4.15	10	4.14	4
3.90	40	3.90	15
3.82	30	3.81	21
3.54	40	3.52	21
		3.48	29
3.37	10	3.36	6
3.20	15	3.19	8
3.01	15	3.01	8
		2.97	5
2.77	50	2.76	25

The pattern of synthetic material exhibiting a finely prismatic habit was obtained with a Gandolfi camera. The data are compared with those presented by Majzlan *et al.* (2005). Intensities were visually estimated. * indicates lines that cannot be indexed with the unit cell of Majzlan *et al.* (2005).

TABLE 2. CRYSTALLOGRAPHIC AND STRUCTURE-REFINEMENT DETAILS FOR $(H_3O)Fe(SO_4)_2$

a (Å)	4.801(2)	Absorption coefficient	3.115 mm^{-1}
b (Å)	8.271(3)	Unique reflections (I>2σ)	863
c (Å)	8.311(3)	*R*(int)	0.017
α (°)	70.605(6)	Final R_1 (%)	4.9
β (°)	89.959(7)	Final wR_2 (%)	12.8
γ (°)	89.951(7)	GOF	1.064
Vol. ($Å^3$)	311.3(2)	D_{calc} (g/cm^3)	2.85
Z	2	Space group	$P\overline{1}$
F(000)	266	Temperature	298(2) K
Crystal size	0.08 × 0.06 × 0.02 mm		

$R_1 = \Sigma \, | |F_o| - |F_c| | \, / \, \Sigma \, |F_o|$; $wR_2 = \{\Sigma \, [w \, (F_o^2 - F_c^2)^2] \, / \, \Sigma \, [w(F_o^2)^2]\}^{1/2}$ ($w = 1 \, / \, [\sigma^2(F_o^2) + (0.0797P)^2 + 0.96 \, P]$, where $P = [\text{Max} \, (F_o^2, 0) + 2F_c^2] \, / \, 3$).

Data were processed using the Bruker AXS NT SHELXTL software package (version 5.10). The raw intensity-data were converted to structure amplitudes using the program SAINT. Absorption corrections (de Meulenaer & Tompa 1965) were applied using the program SADABS. The crystal fragment is non-merohedrally twinned, and two arrays of diffraction intensities were observed. The Bruker computer package program GEMINI (v. 1.0) was applied, and only the reflections from one twin domain that did not overlap with the second orientation were used to solve the structure. The crystal is triclinic (space group $P\overline{1}$), on the basis of the lack of systematic absences, *E* statistics and successful refinement of the structure. Neutral-atom scattering factors were taken from Cromer & Waber (1974). The structure was solved by direct methods. Full-matrix least-square refinements minimizing the function $\Delta w(F_o^2 - F_c^2)^2$ were applied to the compound. Details of the crystallographic parameters and refinement statistics are listed in Table 2. It was not possible to locate the hydrogen atoms. The largest residual peak and hole in the difference-Fourier synthesis were found to be 1.36 and –0.98 e/$Å^3$, respectively. Crystallographic data, atomic coordinates and equivalent isotropic displacement parameters, bond lengths and angles are given in Table 2 to 4. A table of structure factors is available from the Depository of Unpublished Data on the Mineralogical Association of Canada website [document Hydronium ferric sulfate CM47_625].

TABLE 3. COORDINATES AND DISPLACEMENT PARAMETERS OF ATOMS IN $(H_3O)Fe(SO_4)_2$

	x	*y*	*z*	U_{eq}
Fe	0.7501(1)	0.0115(1)	0.2467(1)	0.014(1)
S(1)	0.2502(3)	0.7902(2)	0.4797(2)	0.014(1)
S(2)	0.7502(3)	0.7811(2)	0.9961(2)	0.012(1)
O(1)	0.4200(15)	0.8648(11)	0.3251(9)	0.020(2)
O(2)	-0.0392(14)	0.8608(11)	0.4418(8)	0.018(2)
O(3)	0.3614(16)	0.8410(11)	0.6200(9)	0.022(2)
O(4)*	0.2830(30)	0.6061(19)	0.5314(19)	0.038(5)
O(5)	0.8658(16)	0.8609(10)	0.1180(9)	0.019(2)
O(6)	0.9283(14)	0.8346(10)	0.8423(9)	0.017(2)
O(7)	0.4666(14)	0.8395(11)	0.9512(9)	0.023(2)
O(8)*	0.7600(50)	0.6020(20)	0.0830(20)	0.017(5)
O(9)	0.7502(7)	0.5031(4)	0.7451(4)	0.022(1)

	U_{11}	U_{22}	U_{33}	U_{12}	U_{13}	U_{23}
Fe	0.005(1)	0.032(1)	0.009(1)	-0.012(1)	0.000(1)	-0.001(1)
S(1)	0.011(1)	0.019(1)	0.011(1)	-0.006(1)	0.001(1)	0.000(1)
S(2)	0.011(1)	0.020(1)	0.007(1)	-0.006(1)	0.000(1)	0.000(1)
O(1)	0.011(4)	0.040(5)	0.011(4)	-0.012(3)	0.004(3)	-0.004(3)
O(2)	0.007(4)	0.039(5)	0.008(4)	-0.009(3)	-0.001(3)	-0.003(3)
O(3)	0.015(5)	0.048(5)	0.008(4)	-0.016(4)	-0.008(3)	0.010(4)
O(5)	0.016(5)	0.032(5)	0.013(4)	-0.013(3)	-0.003(3)	0.003(3)
O(6)	0.005(4)	0.037(5)	0.013(4)	-0.015(3)	0.004(3)	-0.002(3)
O(7)	0.004(4)	0.054(6)	0.008(4)	-0.008(4)	0.000(3)	-0.001(3)
O(9)	0.018(2)	0.026(3)	0.022(2)	-0.009(2)	-0.001(2)	-0.001(2)

* refined isotropically. U_{eq} is defined as one third of the trace of the orthogonalized U_{ij} tensor. The anisotropic displacement factor exponent takes the form: $-2\pi^2[h^2a^{*2}U_{11} + ... + 2\,h\,k\,a^*\,b^*\,U_{12} + ...]$.

Refinement of the Structure of Rhomboclase

A sample of rhomboclase from Alcoparrosa, Chile, was obtained from the Royal Ontario Museum (M32666). A crystal fragment (colorless, plate-shaped, size 0.40 × 0.20 × 0.06 mm) was mounted on a glass fiber with epoxy and cooled to –93°C in a stream of nitrogen gas controlled with a Cryostream Controller 700. Data collection was performed on a Bruker SMART APEX II X-ray diffractometer with graphite-monochromated Mo *K*α radiation (λ = 0.71073 Å), over a θ range of 7.84 – 53.98º. No significant decay was observed during the data collection. Data were processed using the Bruker AXS Crystal Structure Analysis Package (Bruker 2006) including data collection: Apex2, cell refinement: Saint, data reduction: Saint, structure solution: Xprep and Shelxtl, and structure refinement: Shelxtl. Neutral-atom scattering factors were taken from Cromer & Waber (1974). The crystal is orthorhombic, space group *Pnma*, on the basis of systematic absences, *E* statistics and successful refinement of the structure. The structure was solved by direct methods. Full-matrix least-square refinements minimizing the function $\Delta w(F_o^2 - F_c^2)^2$ were applied to the compound. All non-hydrogen atoms were refined anisotropically. The positions for all hydrogen atoms were located from difference-Fourier maps, and their positions were refined without constraints. Convergence to final $R_1 = 0.0258$ and $wR_2 = 0.0683$ for 1010 ($I > 2\sigma_{(I)}$) independent reflections, and $R_1 = 0.0272$ and $wR_2 = 0.0695$ for all 1071 [R(int) = 0.0163] independent reflections, with 93 parameters and 0 restraints or constraints, was achieved. The largest residual peak and hole in the difference-Fourier synthesis were found to be 0.58 and –0.45 e/Å^3, respectively. Crystallographic data, atomic coordinates and equivalent isotropic displacement parameters, bond lengths and angles, anisotropic displacement parameters, hydrogen coordinates and isotropic displacement parameters are given in Table 5 to 9. A table of structure factors is available from the Depository of Unpublished Data on the MAC website [document Rhomboclase CM47_625].

The Structure of $(H_3O)Fe^{3+}(SO_4)_2$

The structure of $(H_3O)Fe(SO_4)_2$ is closely related the structure of $(H_3O)Al(SO_4)_2$ described by Fischer *et al.* (1996) and $NH_4Fe(SO_4)_2$ described by Harlow & Novak

TABLE 4. SELECTED BOND-LENGTHS (Å) AND ANGLES (°) IN $(H_3O)Fe(SO_4)_2$

Fe – O(1)	1.971(8)	O1 – Fe – O2	89.4(3)	O1 – S1 – O2	107.9(4)
Fe – O2	1.966(7)	O1 – Fe – O3	91.4(3)	O1 – S1 – O3	110.1(5)
Fe – O3	1.974(7)	O1 – Fe – O5	88.5(3)	O1 – S1 – O4	107.1(7)
Fe – O5	1.972(7)	O1 – Fe – O6	177.2(3)	O2 – S1 – O3	108.1(4)
Fe – O6	1.982(7)	O1 – Fe – O7	89.8(3)	O2 – S1 – O4	117.4(7)
Fe – O7	1.990(7)	O2 – Fe – O3	91.0(3)	O3 – S1 – O4	106.0(7)
Mean	1.976	O2 – Fe – O5	87.8(3)		
		O2 – Fe – O6	93.4(3)	O5 – S2 – O6	107.4(4)
S1 – O1	1.473(7)	O2 – Fe – O7	179.0(3)	O5 – S2 – O7	109.9(4)
S1 – O2	1.499(7)	O3 – Fe – O5	178.8(3)	O5 – S2 – O8	105.5(9)
S1 – O3	1.465(7)	O3 – Fe – O6	88.9(3)	O6 – S2 – O7	110.0(4)
S1 – O4	1.447(15)	O3 – Fe – O7	89.7(3)	O6 – S2 – O8	112.4(9)
Mean	1.471	O5 – Fe – O6	91.2(3)	O7 – S2 – O8	111.4(11)
		O5 – Fe – O7	91.6(3)		
S2 – O5	1.488(7)	O6 – Fe – O7	87.4(3)		
S2 – O6	1.478(7)				
S2 – O7	1.451(7)	O9 – O8	2.739(7)	O8 – O9 – O8'	119.3(8)
S2 – O8	1.418(17)	O9 – O8'	2.823(7)	O8 – O9 – O4	110.6(8)
Mean	1.459	O9 – O4	2.739(7)	O8' – O9 – O4	103.9(8)

TABLE 5. RHOMBOCLASE: CRYSTALLOGRAPHIC AND STRUCTURE-REFINEMENT DETAILS

a (Å)	9.6870(3)	Absorption coeff. (mm^{-1})	2.070
b (Å)	18.2040(6)	Unique reflections (I > 2σ)	3517
c (Å)	5.4250(2)	Final R_1 (%)	2.6
Vol. (Å^3)	956.66(5)	Final wR_2 (%)	6.8
Z	4	GOF	1.112
F(000)	652	Density (calc.) g/cm^3	2.229
Crystal size	0.40 × 0.20 × 0.06 mm	Space group	*Pnma*
Temp.	120(2) K		

$R_1 = \Sigma \mid |Fo| - |Fc| \mid / \Sigma |Fo|$. $wR_2 = \{\Sigma [w (Fo^2 - Fc^2)^2] / \Sigma [w(Fo^2)^2]\}^{1/2}$
($w = 1 / [\sigma^2(Fo^2) + (0.0797P)^2 + 0.96 P]$, where $P = [\text{Max} (Fo^2, 0) + 2Fc^2] / 3$).

TABLE 6. COORDINATES AND EQUIVALENT ISOTROPIC DISPLACEMENT PARAMETERS OF ATOMS IN RHOMBOCLASE

Atom	*x*	*y*	*z*	U_{eq}
Fe	0	0	0	0.010(1)
S	0.2353(1)	0.0886(1)	0.2923(1)	0.011(1)
O(1)	0.3227(1)	0.0232(1)	0.3417(3)	0.014(1)
O(2)	0.0930(1)	0.0608(1)	0.2482(3)	0.015(1)
O(3)	0.2870(2)	0.1281(1)	0.0780(3)	0.018(1)
O(4)	0.2272(1)	0.1353(1)	0.5114(2)	0.015(1)
Ow(1)	0.4904(2)	0.0903(1)	0.7262(3)	0.015(1)
Ow(2)	0.6334(3)	¼	0.5449(6)	0.033(1)
Ow(3a)	0.3850(3)	¼	0.6056(9)	0.024(1)
Ow(3b)	0.391(2)	¼	0.480(6)	0.024(1)
H(1)	0.428(3)	0.0965(2)	0.817(5)	0.031(8)
H(2)	0.565(4)	0.1015(2)	0.787(6)	0.039(9)
H(3)	0.681(4)	0.2131(2)	0.510(6)	0.045(6)
H(4)	0.337(3)	0.2105(2)	0.552(6)	0.045(6)
H(5)	0.495(4)	¼	0.56(1)	0.045(6)

U_{eq} is defined as one third of the trace of the orthogonalized U_{ij} tensor.

TABLE 7. ANISOTROPIC DISPLACEMENT PARAMETERS (Å^2) FOR RHOMBOCLASE

	U_{11}	U_{22}	U_{33}	U_{12}	U_{13}	U_{23}
Fe	0.009(1)	0.015(1)	0.008(1)	0.001(1)	0.000(1)	–0.001(1)
S	0.009(1)	0.015(1)	0.008(1)	0.000(1)	0.000(1)	0.000(1)
O(1)	0.011(1)	0.017(1)	0.014(1)	0.001(1)	0.003(1)	–0.001(1)
O(2)	0.010(1)	0.024(1)	0.012(1)	–0.005(1)	0.002(1)	–0.001(1)
O(3)	0.019(1)	0.021(1)	0.012(1)	0.005(1)	–0.005(1)	–0.002(1)
O(4)	0.013(1)	0.019(1)	0.012(1)	–0.005(1)	0.000(1)	0.002(1)
Ow(1)	0.013(1)	0.021(1)	0.012(1)	–0.003(1)	0.001(1)	–0.002(1)
Ow(2)	0.022(1)	0.018(1)	0.060(2)	0	0.010(1)	0
Ow(3a)	0.023(1)	0.017(1)	0.032(3)	0	–0.004(1)	0
Ow(3b)	0.023(1)	0.017(1)	0.032(3)	0	–0.004(1)	0

The anisotropic displacement factor exponent takes the form: $-2\pi^2[\, h^2 a^{*2} U_{11} + ... + 2\, h\, k\, a^*\, b^*\, U_{12} + ...]$.

TABLE 8. BOND LENGTHS (Å) AND ANGLES (°) IN RHOMBOCLASE

Fe – O(1)	1.966(1) ×2	O(2)–Fe(1)–O(1)	91.12(5)	O(1)–S(1)–O(2)	106.43(8)
Fe – O(2)	1.962(1) ×2	O(2)–Fe(1)–O(1)	88.88(5)	O(3)–S(1)–O(1)	110.12(8)
Fe – Ow(1)	2.053(2) ×2	O(2)–Fe(1)–Ow(1)	88.83(6)	O(4)–S(1)–O(1)	110.48(8)
Mean	1.994	O(2)–Fe(1)–Ow(1)	91.17(6)	O(3)–S(1)–O(2)	111.04(9)
		O(1)–Fe(1)–Ow(1)	87.15(6)	O(4)–S(1)–O(2)	106.18(8)
S – O(1)	1.486(1)	O(1)–Fe(1)–Ow(1)	92.85(6)	O(3)–S(1)–O(4)	112.36(9)
S – O(2)	1.488(1)				
S – O(3)	1.456(1)				
S – O(4)	1.463(1)				
Mean	1.473				

TABLE 9. HYDROGEN BONDS (Å) AND ANGLES (°) FOR RHOMBOCLASE

D–H...A	d(D–H)	d(H...A)	d(D...A)	<(DHA)
Ow(3a)–H(5).....Ow(2)	1.10(4)	1.34(4)	2.429(4)	169(5)
Ow(3b)–H(5).....Ow(2)	1.10(4)	1.34(4)	2.38(2)	155(5)
Ow(1)–H(1).....O(3)	0.79(3)	2.05(3)	2.828(2)	169(3)
Ow(2)–H(3).....O(3)	0.84(3)	1.92(3)	2.753(2)	179(3)
Ow(1)–H(2).....O(4)	0.82(3)	2.01(3)	2.821(2)	170(3)
Ow(3a)–H(4).....O(4)	0.90(3)	1.75(3)	2.637(2)	167(3)
Ow(3b)–H(4).....O(4)	0.97(3)	1.75(3)	2.63(1)	149(4)

(2004). Both exhibit space group $R\bar{3}$ with a 4.711(2), c 23.254(4) Å for $(H_3O)Al(SO_4)_2$ and a 4.8275(2), c 24.40(9) Å for $NH_4Fe(SO_4)_2$. Within the unit cell of $(H_3O)Al(SO_4)_2$, there are three layers with an interlayer spacing of 7.75 Å. The layers consist of $Al(SO_4)_2$ sheets parallel to (001) composed of AlO_6 octahedra and SO_4 tetrahedra sharing corners (Fig. 3a). Each SO_4 tetrahedron is linked to three AlO_6 octahedra, and every corner of each Al octahedron is connected to a SO_4 tetrahedron. These layers are similar to the layer structure found in many compounds including merwinite, $Ca_3Mg(SiO_4)_2$ (Moore & Araki 1972), in which the MgO_6 octahedra share corners with SiO_4 tetrahedra, and yavapaiite (Graeber & Rosenzweig 1971), in which the FeO_6 octahedra share corners with sulfate tetrahedra. Fleck & Kolitsch (2003) pointed out that these structures can be described as sheets made up of kröhnkite-type chains with composition $[M(XO_4)_2(H_2O)_2]$.

In $(H_3O)Al(SO_4)_2$, the oxygen of the H_3O group is located at site 3b, which has site-symmetry $\bar{3}$, and the H_3O molecule, which has symmetry 3m, is disordered with respect to orientation to maintain an average overall symmetry of $R\bar{3}$ (Fig. 3b). Hydrogen bonds form between the hydrogen atoms of the H_3O molecule and the oxygen atoms of the sulfate groups on adjacent layers to create a continuous layer of orientationally disordered H_3O molecules (Fig. 3b). The O–H...O separation is 2.84 Å. The H position was not observed in refinement of the X-ray-diffraction data. The spacing of the oxygen atoms of the array formed by the apices of the sulfate tetrahedra is 4.71 Å, and the Al–O bond length is 1.897 Å (Fischer *et al.* 1996). In $NH_4Fe(SO_4)_2$, the NH_4 groups are also positionally disordered (Harlow & Novak 2004).

The structure of $(H_3O)Fe(SO_4)_2$ is distorted from the $R\bar{3}$ arrangement of $(H_3O)Al(SO_4)_2$ to $P\bar{1}$ symmetry; it has a layer spacing of 7.90 Å, which is slightly larger than the spacing for $(H_3O)Al(SO_4)_2$ (7.75 Å). This increase is a direct result of the mean $^{VI}Fe^{3+}$–O bond length (1.98 Å) being longer than the Al–O bond length (1.879 Å). The longer ^{VI}Fe–O bond length causes the array of oxygen atoms formed by the apices of the sulfate groups that bond to the hydronium groups to be farther apart. This increases the O_D–H...O_A separation between the hydronium oxygen (donor) and the sulfate oxygen (acceptor). In order to maximize the strength of the hydrogen bonds, the sulfate tetrahedra tilt with respect to the layer. In $(H_3O)Al(SO_4)_2$, all of the O_D–H...O_A distances are equal (Fig. 3b), and the hydronium is positionally disordered over two orientations allowed by the $\bar{3}$ symmetry. In $(H_3O)Fe(SO_4)_2$, because of the sulfate tilting, the symmetry becomes $P\bar{1}$, and four of the O_D–H...O_A bonds are shorter and two are longer. Figures 3c and 3d show the tilting of the tetrahedra, which results in the H_3O groups forming hydrogen bonds in a chain-like arrangement rather than as a sheet, as seen in $(H_3O)Al(SO_4)_2$. In the more symmetrical $R\bar{3}$ structure of $(H_3O)Al(SO_4)_2$, the H_3O molecule is disordered over two different orientations.

The oxygen atom of the hydronium group forms hydrogen bonds with the underbonded apical oxygen atoms of the sulfate tetrahedra. The hydrogen atom positions could not be determined; the presence of hydrogen bonds is inferred from the composition of the material and the distances between non-hydrogen atoms. These hydrogen bonds connect to apical oxygen atoms of sulfate tetrahedra in the same layer (Fig. 3c). The O...O separations, 2.739, 2.739 and 2.823 Å, and the average O–O–O angle, 111° (Table 4), are consistent with distances and angles of a location where a hydronium group could be situated, as summarized by Bell (1973), and the molecular geometry of H_2O described by Chiari & Ferraris (1982). There is a fourth possible O_D–H...O_A bond, shown as a dotted line in Figure 3c. The distance of 2.81 Å is within the range observed for

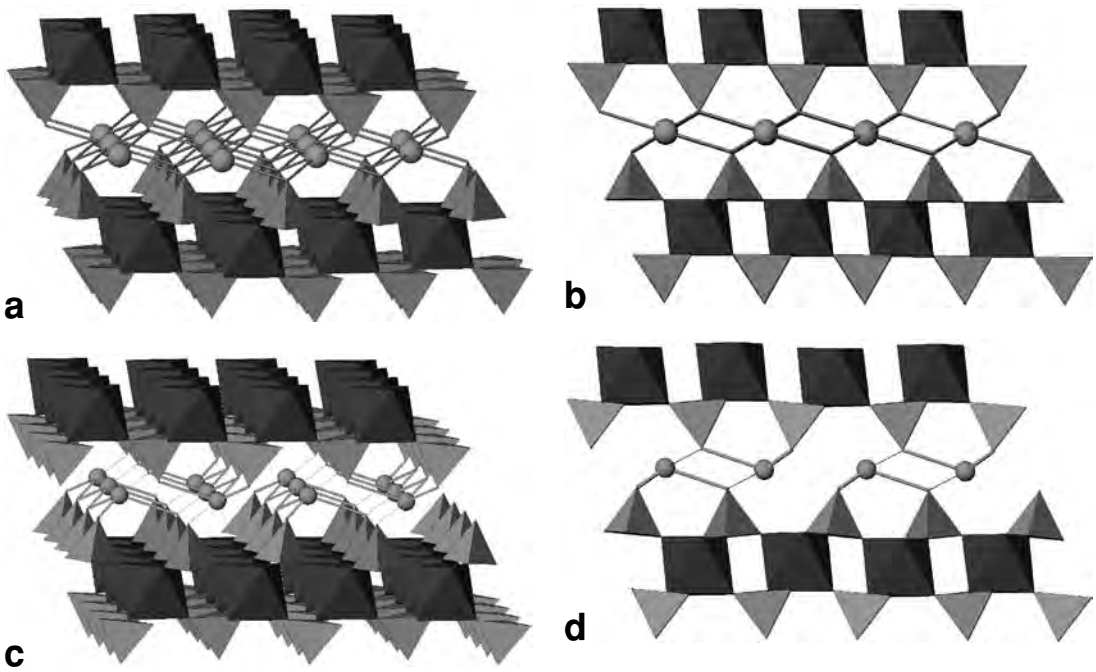

FIG. 3. a) The structure of $(H_3O)Al(SO_4)_2$ is composed of sheets of AlO_6 octahedra, perpendicular to (001) linked by SO_4 tetrahedra. Every corner of each octahedron is shared with a sulfate tetrahedron, and the structure has $R\bar{3}$ symmetry. b) The planar layers, as seen looking down the *a* axis, are held together by H_3O molecules evenly distributed between the sheets, and are positionally disordered. c, d) In $(H_3O)Fe(SO_4)_2$, the increased size of the FeO_6 octahedra requires that the SO_4 tetrahedra tilt to maintain reasonable H–O...H distances (viewed down *a*). The symmetry of the structure is reduced from $R\bar{3}$ to $P\bar{1}$, and the H_3O molecules form linear arrays rather than disordered sheets.

O_D–H...O_A bonds, but if this were an O_D–H...O_A bond, the H–O–H angle within the H_3O molecule must be close to 60° or 180°, which is not possible.

The distortion of the structure of $(H_3O)Fe(SO_4)_2$ results in distances between adjacent H_3O groups being the shortest in the *a* direction. This suggests that if protonic conduction occurs, it will take place along this direction and not throughout the sheet as for $(H_3O)Al(SO_4)_2$ (Fischer *et al*. 1996). The additional O_D–H...O_A separation may also play a role in affecting the protonic conduction.

In $(H_3O)Fe(SO_4)_2$, the stacking of the layers is not as symmetrical as in $(H_3O)Al(SO_4)_2$. The layers are staggered, and the lower symmetry $P\bar{1}$ results. This distortion of a rhombohedral symmetry explains the twinning observed for this material. Because of the trigonal symmetry of the sheets, there are three energetically similar directions of distortion related by 60° in the (001) plane. The distortion that results from the hydrogen bonding lowers the symmetry. In an adjacent part of the crystal, this distortion may have taken place about one of the other possible directions, resulting in a twinned relationship between the two domains. In Figure 2, the three different optical orientations of a trilling may be seen in cross-polarized light. This stacking system based on a triclinic (pseudomonoclinic) offset of a hexagonal sheet is similar to that seen for micas. Using the nomenclature developed for micas, $(H_3O)Fe(SO_4)_2$ would be a 1*T* polytype. It is possible that other polytypes of the $(H_3O)Fe(SO_4)_2$ structure exist.

The layers are held together by weak hydrogen bonding. This is consistent with the observation that on exposure to a humid atmosphere after growth, the crystals expand to resemble a "wet book" as molecules of water are incorporated between the layers, and the material becomes amorphous. Whether $(H_3O)Fe(SO_4)_2$ will crystallize if the humidity is lowered or whether rhomboclase will form instead in not known.

THE STRUCTURE OF RHOMBOCLASE

The structure determination of rhomboclase, $(H_5O_2)Fe(SO_4)_2 \bullet 2H_2O$, as described here, confirms the earlier model of Mereiter (1974). The structure is composed of layers of FeO_6 octahedra linked by SO_4 tetrahedra parallel to (010), with a layer spacing of 8.3 Å (Fig. 4). In the layers, each octahedron is linked to four sulfate tetrahedra, and each tetrahedron links two Fe octahedra.

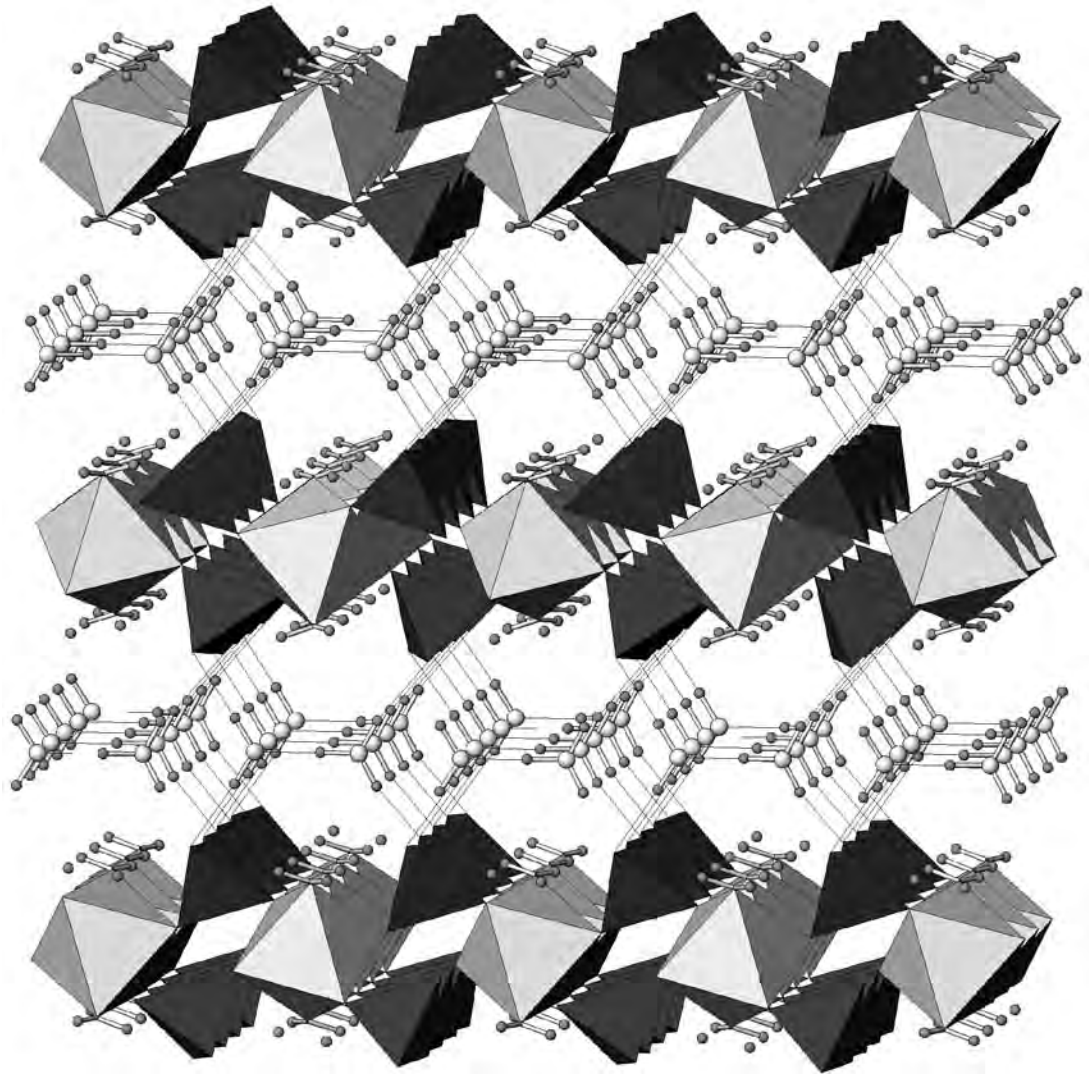

FIG. 4. The structure of rhomboclase $(H_5O_2)Fe(SO_4)_2•2H_2O$ is composed of sheets of $Fe(SO_4)_2•2H_2O$ parallel to (010) that are held together by hydrogen bonds with H_5O_2 groups. The layer spacing is 8.3 Å. The chains of edge-sharing FeO_6 octahedra are parallel to the *a* axis.

Only two of the sulfate oxygen atoms are involved with links to FeO_6 octahedra, unlike $(H_3O)Fe(SO_4)_2$, where three are involved in links to FeO_6 octahedra. In rhomboclase, only four out of the six octahedron vertices are involved in linkages, whereas in $(H_3O)Fe(SO_4)_2$, each vertex of a FeO_6 octahedron is involved in a link with sulfate tetrahedra. The two vertices of the FeO_6 octahedron in rhomboclase that are not bonded to a sulfate tetrahedron are occupied by H_2O molecules.

The additional H_2O molecules are located between the layers (Fig. 5). Atoms Ow3a and Ow2 of the H_2O_5 group are separated by 2.429(4) Å. Atom Ow3 is bonded to two symmetrically equivalent H4 atoms at 0.90 Å that form an H–O–H angle of 105.3°. Atom Ow2 is bonded to two symmetrically equivalent H3 atoms at 0.84 Å that form an H–O–H angle of 106.8°. A difference-Fourier calculation reveals a peak in electron density between Ow3a and Ow2, 1.10 Å from Ow3a and 1.34 Å from Ow2. This geometry is very close to that observed for H_5O_2 in $(H_5O_2)In(SO_4)_2•2H_2O$, where the O...O separation is 2.41(2) (Tudo *et al.* 1979). Theoretical calculations of the most stable conformation of

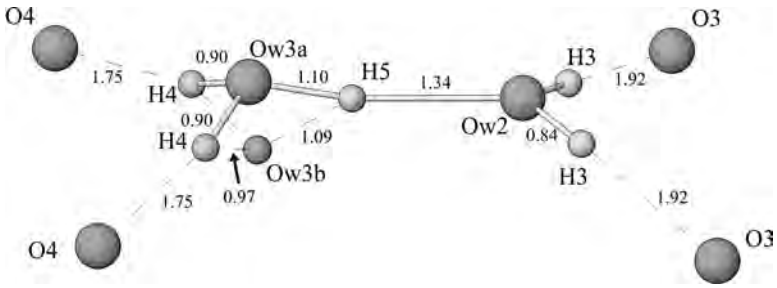

FIG. 5. Hydrogen bonds (Å) of the H_5O_2 molecule in rhomboclase. The Ow3a position has an occupancy of 86% (*trans* configuration), and Ow3b has an occupancy of 14% (*cis* configuration).

the H_5O_2 molecule by Newton & Ehrenson (1971) indicate the O...O separation to be 2.36 Å, with an H–O–H angle of 115°. The difference-Fourier calculation also reveals a peak close to Ow3a that is interpreted to be a partially occupied oxygen site of a second configuration of the H_5O_2 molecule. The hydrogen atoms that surround Ow2 form a trigonal pyramidal arrangement. Those that surround Ow3a also form a trigonal pyramidal arrangement, and this pyramid points in the same direction as the coordination around Ow2 to form a H_5O_2 molecule in a *cis* configuration. The trigonal pyramidal coordination of Ow3b points in the opposite direction and creates a molecule with a *trans* configuration. Site-occupancy refinements of these sites indicate that the *cis* configured molecule described by Ow3a and Ow2 is present in 86% of the sites, and the molecule described by Ow3b and Ow2 is present in 14% of the sites. This positional disorder of the H_5O_2 group was also observed by Mereiter (1974), but hydrogen positions were inferred and not observed. This disorder may be static or dynamic, but this cannot be discriminated by the single-crystal X-ray-diffraction experiment.

Table 10 presents the bond-valence calculation for rhomboclase. For simplicity, the calculation assumes 100% occupancy of the Ow3a position. Refined atomic positions for hydrogen obtained by X-ray diffraction give O–H bonds that are shorter than the true O–H separation (Shannon 1976) because of the covalent nature of the electron distribution. This is overcome by assuming that O–H bonds shorter than 0.97 Å should be modeled as 0.97 Å. In the case of the bond to H5, which is longer than 0.97 Å, it is not necessary to make this assumption. Table 10 shows that the bond valence is evenly distributed throughout the structure.

TABLE 10. BOND-VALENCE SUMS (*vu*) FOR RHOMBOCLASE

	O1	O2	O3	O4	Ow1	Ow2	Ow3	Cation sum
Fe1	0.5675	0.5741			0.4434			
	1.1350	1.1483			0.8868			3.17
S1	1.4270	1.4191	1.5510	1.5211				
	1.4270	1.4191	1.5510	1.5211				5.92
H1			0.1517		0.7871			
			0.1517		0.7871			0.94
H2				0.1585	0.7871			
				0.1585	0.7871			0.95
H3			0.1753			1.5743		
			0.1753			0.7871		0.96
H4				0.2149			1.5743	
				0.2149			0.7871	1.00
H5						0.3866	0.5969	
						0.3866	0.5969	1.00
Anion sum	1.99	1.99	1.88	1.90	2.02	1.96	2.17	

The parameters used in the calculation are taken from Brown (1981). The upper entry in each pair is the sum of the valence units from the cation to the anion. The lower entry is the sum of the valence units arriving at the cation from the anion. Contributions from hydrogen atoms are calculated on the basis of a typical O–H distance of 0.97 Å in H_2O groups (Shannon 1976). The calculations of valence units involving H5 used the observed O–H distance, as it is longer than 0.97 Å.

ACKNOWLEDGEMENTS

This work was supported by a NSERC Discovery grant to R.C.P. We thank Robert Ramik of the Royal Ontario Museum for providing the specimen of rhomboclase. We thank M. Schindler and M. Fleck for constructive reviews, and U. Kolitsch for a constructive review and editorial assistance.

REFERENCES

BELL, R.P. (1973): *The Proton in Chemistry* (2nd ed.). Cornell University Press, Ithaca, New York.

BRACH, I., JONES, D.J. & ROZIERE, J. (1989): Acid sulphates of trivalent metals: a new class of protonic conductors. *Solid State Ionics* **34**, 181-185.

BROWN, I.D. (1981): The bond-valence method: an empirical approach to chemical structure and bonding. *In* Structure and Bonding in Crystals (M. O'Keeffe & A. Navrotsky, eds.). Academic Press, New York, N.Y. (1-30).

BRUKER AXS INC. (2006): Bruker AXS Crystal Structure Analysis Package Madison, Wisconsin.

CHANG, F.M., JANSEN, M. & SCHMITZ, D. (1983): Structure of pentahydrogendioxygen(1+) diaquadisulfatomanganate(III), $[H_5O_2]^+[Mn(H_2O)_2(SO_4)_2\}^-$. *Acta Crystallogr.* **C39**, 1497-1498.

CHIARI, G. & FERRARIS, G. (1982): The water molecule in crystalline hydrates studied by neutron diffraction. *Acta Crystallogr.* **B38**, 2331-2341.

CROMER, D.T. & WABER, J.T. (1974): *International Tables for X-ray Crystallography*. Kynoch Press, Birmingham, U.K. (Vol. 4, Table 2.2 A).

FISCHER, T., EISENMANN, B. & KNEIP, R. (1996): Crystal structure of oxonium bis(sulfato) aluminate $H_3O[Al(SO_4)_2]$. *Z. Kristallogr.* **121**, 465.

FLECK, M. & KOLITSCH, U. (2003): Natural and synthetic compounds with the kröhnkite-type chains. An update. *Z. Kristallogr.* **218**, 553-567.

GLASSER, L. (1977): Proton conduction and injection in solids. *Chem. Rev.* **75**, 21-45.

GRAEBER, E.J. & ROSENZWEIG, A. (1971): The crystal structures of yavapaiite, $KFe(SO_4)_2$, and goldichite, $KFe(SO_4)_2 \cdot 4H_2O$. *Am. Mineral.* **56**, 1917-1933.

HASHMI, S.A., RAI, D.K. & CHANDRA, S. (1992): Protonic conduction in $Al_2(SO_4)_3 \cdot 16H_2O$: coulometry, transient ionic current, infrared and electrical conductivity studies. *J. Mater. Sci.* **27**, 175-179.

HARLOW, R.L. & NOVAK, J.M. (2004): Iron ammonium bis (sulfate) as a by-product of aniline production. Private communication, 413817. Inorganic Structure Database, Fachinformationszentrum Karlsruhe, Germany.

LAUSEN, C. (1928): Hydrous sulphates formed under fumerolic conditions at the United Verde mine. *Am. Mineral.* **13**, 203-229.

MAJZLAN, J., BOTEZ, C. & STEPHENS, P.W. (2005): The crystal structure of synthetic $Fe_2(SO_4)_3(H_2O)_5$ and the type specimen of lausenite. *Am. Mineral.* **90**, 411-416.

MAJZLAN, J., NAVROTSKY, A., MCCLESKEY, R.B. & ALPERS, C.N. (2006): Thermodynamic properties and crystal structure refinement of ferricopiapite, coquimbite, rhomboclase, and $Fe_3(SO_4)_2(H_2O)_5$. *Eur. J. Mineral.* **18**, 175-186.

MARGULIS, E.V., SAVCHENKO, L.A., SHOKAREV, M.M., BEISEKEEVA, L.I. & KAPATSINA, G.A. (1973): Basic iron sulfate in the $Fe_2(SO_4)_3$ acetone–water system. *Russ. J. Inorg. Chem* **18**, 1128-1132.

MEREITER, K. (1974): Die Kristallstruktur von Rhomboklas $H_5O_2Fe(SO_4)_2 \cdot 2H_2O$. *Tschermaks Mineral. Petrogr. Mitt.* **21**, 216-232.

DE MEULENAER, J. & TOMPA, H. (1965): The absorption and extinction correction in crystal structure analysis. *Acta Crystallogr.* **19**, 1014-1018.

MOORE, P.B. & ARAKI, T. (1972): Atomic arrangement of merwinite, $Ca_3Mg(SiO_4)_2$, an unusual dense-packed structure of geophysical interest. *Am. Mineral.* **57**, 1355-1374.

MORRIS, R.V., MING, D.W., CLARK, B.C., KLINGELHÖFER, G., GELLERT, R., RODIONOV, D., SCHRÖDER, C., DE SOUZA, P. & YEN, A. (2005): Abundance and speciation of water and sulfate at Gusev crater and Meridiani Planum. *Lunar and Planet. Sci. Conf.* **XXXVI**, 2239 (abstr.).

NEWTON, M. D. & EHRENSON, S. (1971): *Ab initio* studies on the structures and energetics of inner- and outer-shell hydrates of the proton and hydroxide ion. *J. Am. Chem. Soc.* **93**, 4971-4990.

PALACHE, C., BERMAN, H. & FRONDEL, C. (1951): *The System of Mineralogy* (seventh ed.). John Wiley & Sons, New York, N.Y. (1124).

PONOMAREVA, V.G., BURGINA, E.B., TARNOPOLSKY, V.A. & YAROSLAVTSEV, A.B. (2002): Proton mobility in the composites of iron acid sulfate monohydrate with silica. *Mendeleev Commun.* **12**, 223-224.

POSNJAK, E. & MERWIN, H.E. (1922): The system $Fe_2O_3 – SO_3 – H_2O$. *J. Am. Chem. Soc.* **44**, 1965-1994.

SHANNON, R.D. (1976): Revised effective ionic radii and systematic studies of interatomic distances in halides and chalcogenides. *Acta Crystallogr.* **A32**, 751-767.

SREBRODOLSKIY, B.L. (1974): Lausenite, first find in the USSR. *Dokl. Akad. Nauk SSSR* **219**, 125-126.

TROJANOV, S., STIEWE, A. & KEMNITZ, E. (1996): Synthese und Struktur saurer Übergangsmetallsulfate $Ti(H_5O_2)(SO_4)_2(H_2O)_2$ und $Zr(H_3O)_2(SO_4)_3$. *Z. Naturforsch.* **51B**, 19-24.

TUDO, J., JOLIBOIS, B., LAPLACE, G., NOWOGROCKI, G. & ABRAHAM, F. (1979): Structure cristalline du sulfate acide d'indium(III) hydraté. *Acta Crystallogr.* **B35**, 1580-1583.

Received August 31, 2007, revised manuscript accepted May 17, 2009.